Langmuir

Article

pubs.acs.org/Langmuir

Impact of Membrane Fluidity on Steric Stabilization by Lipopolymers

Raquel Orozco-Alcaraz and Tonya L. Kuhl*

Department of Chemical Engineering and Materials Science, University of California, Davis, One Shields Avenue, Davis, California 95616, United States

ABSTRACT: In this work, the impact of lipid lateral mobility on the steric interaction between membranes containing poly(ethylene glycol) (PEG) functionalized lipids was investigated using the surface force apparatus. The force−distance profiles show the presence of electrostatic and steric repulsion that arise from the presence of negatively charged PEG functionalized lipids. Fluid-phase bilayers have high lateral diffusion relative to gel-phase bilayers; however, a quantitative comparison of the interaction forces between membranes in these two different phase states demonstrates a reduced rate of diffusion in the fluid phase for the PEG-lipids under constrained geometries. Thus, the amount of polymer in the contact zone can be modulated and is reduced with fluid membranes; however, complete exclusion was not achieved. As a result, the steric repulsion afforded by PEG chains or binding affinity of ligated PEG chains can only be modestly tailored by the phase state of the liposome.

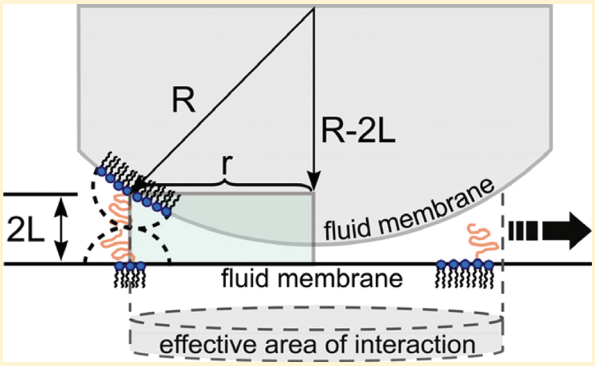

INTRODUCTION

Because of its low toxicity, low protein absorption, nonionic character, and solubility in both aqueous and organic solvents, poly(ethylene glycol) (PEG) is the most commonly used polymer coating to biocompatibilize surfaces for biomedical applications.[1−6] One specific application involves the grafting of PEG to vesicle or liposome surfaces for drug delivery. By judicious choice of grafting density and PEG molecular weight, circulation half-lives of liposomes can be extended from hours to days due to reduced plasma interactions by the steric repulsive barrier presented by the polymer chains.[7−13] As a result, PEG-coated liposomes have acquired the moniker "Stealth Liposomes" due to their ability to evade the body's immune system. The enhanced circulation time allows Stealth Liposomes to accumulate inside tissues and tumors, which leads to a drug-release system referred to as passive targeting.[10]

However, extending circulation times is only part of the equation. It is also highly desirable to actively target the liposome to a specific diseased cell type, e.g., cancer cells. Toward this goal, there has been significant effort to functionalize PEG chains with specific ligands to provide selective targeting.[10,14−18] In ex vivo studies such as cell culture, selective targeting has been demonstrated to work with high efficiency.[19] Unfortunately, translating these benchtop studies to animals or humans has not demonstrated significant benefit or increase in efficacy through targeting. While many studies of liposomal based technologies look promising, PEGylated liposomal doxorubicin (DOXIL/Caelyx) has been the only approved liposomal formulation in the USA and Europe for Kaposi's sarcoma and recurrent ovarian cancer.[20−22]

PEG steric stabilization clearly aids in circulation longevity, but it can also be viewed as a steric hindrance once the liposome reaches the active site.[5] It has been reported that reducing steric repulsion increases the net adhesive force of ligands to access receptor sites.[16] Though different formulations have been created to increase the binding effectiveness in targeting, it is important to understand the surface behavior of a PEGylated membrane when it comes into contact with another surface. Here, we investigate the impact of membrane fluidity and lateral mobility of PEG functionalized lipids on the steric interaction between two opposing membranes. In this system, the grafting density of the PEG chains in the contact region can dynamically respond to confinement and diffuse along the lipid membrane surface. Consequently, fluidity can reduce steric hindrance once the liposomal surface reaches the target site. The measured reduction in the steric interaction is used to estimate the diffusion of the PEG functionalized lipids in the contact region between the opposing membranes.

MATERIALS AND METHODS

Chemicals. 1,2-Dipalmitoyl-*sn*-glycero-3-phosphoethanolamine (DPPE), 1,2-dimyristoyl-*sn*-glycero-3-phosphocholine (DMPC), and 1,2-dimyristoyl-*sn*-glycero-3-phosphoethanolamine-*N*-[methoxy-(polyethylene glycol)-2000] (ammonium salt) (DMPE-PEG2000) were purchased from Avanti Polar Lipids, Inc. (Alabaster, AL) and used as received.

Sample Preparation. Supported lipid bilayers were prepared by Langmuir−Blodgett (LB) deposition using a temperature-controlled Wilhelmy Trough (Nima Coventry, UK) as described elsewhere.[23,24] Lipids were dissolved in 9:1 chloroform/methanol at a concentration of approximately 1 mg/mL. The bilayer surfaces were assembled onto

Received: February 28, 2012
Revised: April 21, 2012
Published: April 26, 2012

   dx.doi.org/10.1021/la3008552 | *Langmuir* 2012, 28, 7470−7475

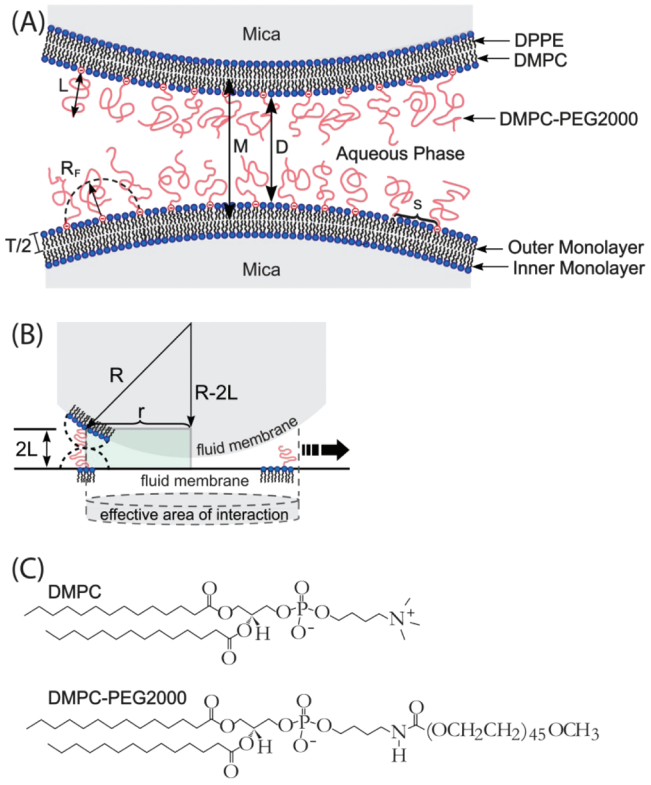

Figure 1. (A) Illustration of the lipopolymer bilayer geometry in the SFA. R_F denotes the Flory radius of the polymer chain, which is 35 Å for PEG-2000.[23,24] The average distance between PEG grafting sites is symbolized by s, where $\sigma = s^{-2}$ and σ is the lipopolymer-grafting density in the outer layer. M is the distance based on the contact between the inner DPPE monolayers, $T/2$ is the outer DMPC layer thickness, and L is the polymer layer thickness. $D = 0$ is defined as the contact between two "nominally" dehydrated bilayers, $D = M - T$. (B) Illustration of maximum distance, r, a lipopolymer needs to travel in order to exit the contact zone between two surfaces. R is the radius of curvature of the cylindrical support surface ($R \gg 2L$). (C) Chemical structures of the molecules used for the outer leaflet shown in part A.

molecularly smooth, back-silvered mica substrates glued onto silica disks (Figure 1). A close-packed, solid-phase inner monolayer of DPPE (~43 Å^2 per molecule, Π = 40 mN/m) was first deposited by raising the substrates vertically through a compressed DPPE monolayer at the air–water interface yielding transfer ratios of 1.0 ± 0.05. Afterward, an outer layer of 92.5 mol % DMPC + 7.5 mol % DMPE-PEG2000 was deposited onto the DPPE film at 35 mN/m. The transfer ratios of the mixed outer monolayers were 0.99 ± 0.03. DMPC was chosen as the matrix lipid because its phase transition temperature is 23.5 °C;[25] thus, the temperature of the system can be easily manipulated to modify the diffusivity of the outer lipid layer; below 23.5 °C in the solid phase D ~0.02 μm^2/s[26] and above in the fluid phase D ~4 μm^2/s.[27]

Surface Force Measurements. The surface force apparatus (SFA) was used to measure the interaction forces between the PEGylated bilayers. The SFA technique has been used extensively to measure interaction forces between surfaces.[28,29] The studies using this method provide a better understanding for intersurface behavior between relatively large areas, compared to atomic force microscopy (AFM) performed in previous studies.[30] After depositing the membranes on mica, the surfaces were transferred and mounted into the SFA under water, a procedure detailed elsewhere.[31] The water in the SFA box was saturated with a speckle of DMPC to prevent lipid desorption from the solid substrate. After the surfaces were mounted, the SFA box was placed in a temperature-controlled room at 20 °C, which is below DMPC's transition temperature. To measure the interacting forces when in the fluid phase, the temperature was later increased to 28 °C. A custom automated SFA was used for convenient data collection.[17] The system enabled constant surface displacement via a computer-controlled motor system. A sensitive CCD camera was interfaced with the spectrometer and computer acquisition system to allow automated wavelength determination of the fringes of equal chromatic order.

Bilayer–bilayer contact, D = 0, was defined as the contact between nominally dehydrated bilayers without any polymer layer.[23] Both PC and PE lipids are zwitterionic. However, PEG-functionalized lipids are negatively charged as the PEG chain is covalently attached to the terminal amine headgroup of the DMPE lipid. Any electrostatic interaction between the membrane surfaces is therefore attributed to the presence of DMPE-PEG2000 (Figure 1). As the negative charge is at the phosphate group, the outer Helmholtz plane in the electrostatics analysis used the same reference of D = 0 as in the force profile measurements.

RESULTS AND DISCUSSION

Isotherms for the various lipid monolayers, 100% DMPC, 100% DMPE-PEG2000, and 7.5 mol % DMPE-PEG2000 + 92.5 mol % DMPC, are shown in Figure 2. Lateral interactions between

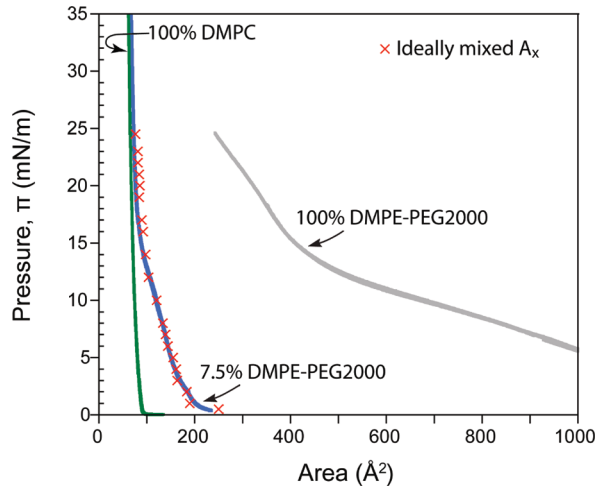

Figure 2. Surface pressure vs area curve isotherms of: 100 mol % DMPC, 100 mol % DMPE-PEG2000, and 7.5 mol % DMPE-PEG2000 + 92.5 mol % DMPC. Symbols (x) are the theoretical prediction if the mixture behaves ideally.

lipids and PEGylated lipids in monolayers at the air–water interface have been previously measured. It has been reported that, above a critical pressure of ~10 mN/m, it is energetically more favorable for the polymer to extend into the water solution, and that lipopolymer mixes with the lipid at the air–water interface.[24,32] In this work with DMPC doped DMPE-PEG2000 monolayers, we observe the same phenomenon of PEG absorbed to the air–water interface and then squeezed into the water subphase with increasing lateral compression. To establish whether DMPC and DMPE-PEG2000 phase separate or mix, the isotherm of the monolayer doped with 7.5 mol % DMPE-PEG2000 was compared to that expected for ideal-mixed behavior, expressed by eq 1

$$A_x = xA_P + (1 - x)A_L \quad (1)$$

Here, A_x is the average area of a molecule in mixture at the air–water interface, A_L is the area of a DMPC lipid in a pure

dx.doi.org/10.1021/la3008552 | Langmuir 2012, 28, 7470–7475

monolayer, A_P is the area of a PEG2000 chain in a pure DMPE-PEG monolayer, and X is the mole fraction of DMPC in the mixed monolayer. The x-points curve in Figure 2 displays A_x as a function of surface pressure, where A_L and A_P were obtained from the pure DMPC and DMPE-PEG2000 isotherms, respectively. The A_x curve overlaps the isotherm obtained experimentally demonstrating that the system mixes ideally. As a result, the grafting density of the lipopolymer is readily obtainable from the mol % of lipopolymer and the area per lipid molecule. At 35 mN/m, the average area per molecule is 57 Å^2, a value consistent with previous measurements.[33] Thus, for the 92.5 mol % DMPC/7.5 mol % DMPE-PEG monolayer, the area per grafted PEG chain, σ, is ~760 Å^2, yielding a distance, s, of ~28 Å between grafting points. Relative to the unperturbed polymer chain radius of gyration, $R_F = \alpha N^{0.6} = 35$ Å, this grafting density is in the overlapping mushroom regime, $\sigma^* = R_F^2/\sigma \approx 1.7$.[23,24,34] A 7.5 mol % concentration was selected to match the grafting density of previously studied 4.5–5 mol % DSPE-EO_{45} mixed in gel-phase DSPE membranes.[23,24] DSPE has a molecular area of 43 Å^2 yielding a lipo-polymer area of 860 Å^2 or s ~29 Å for these gel-phase studies.

Figure 3 shows an example force–distance profile between two DMPC bilayers doped with 7.5 mol % DMPE-PEG2000 at

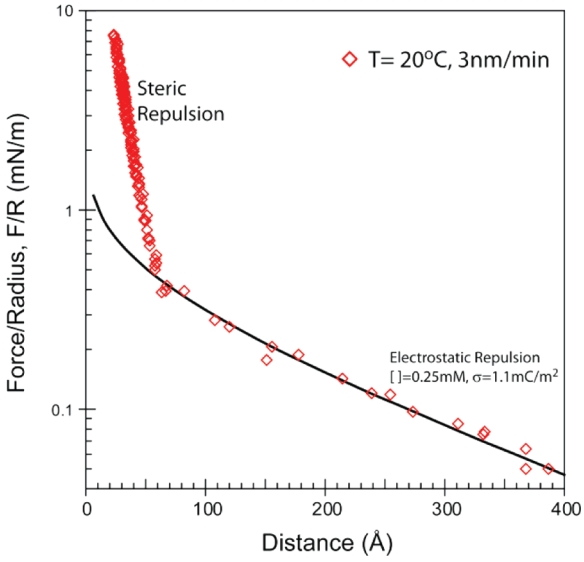

Figure 3. Force–distance profile of DMPC bilayers with a surface coverage of 7.5% DMPE-PEG2000 at 20 °C. The electrostatic curve was fit using the concentration of [$NaNO_3$] = 0.25 mM and surface charge density of 1.1 mC/m^2.

20 °C. At this temperature, the membrane is in the gel phase and the force profile closely matches the results obtained with gel-phase membranes containing 4.5–5 mol % DSPE-PEG2000.[23,24] As expected, the force–distance curve displays long-range electrostatic and shorter-range steric repulsion associated with the presence of the lipopolymers in the membranes. Theoretically and experimentally, both the electrostatic and steric forces decay roughly exponentially. In the case of electrostatic forces, the decay is determined by the ionic strength (Debye length, κ^{-1} ~200 Å). In the weakly overlapping mushroom regime, the steric interaction has a characteristic decay length approximately the thickness of the polymer layer, $R_F = 35$ Å, but for two layers it would be $2R_F \approx$ 70 Å. Unless the two decay lengths are similar, a double-exponential curve is measured from which the electrostatic and steric contribution can be separated. The electrostatic contribution was determined by solving the nonlinear Poisson–Boltzmann equation explicitly using a numerical algorithm.[35] The solid line in Figure 3 is the electrostatic contribution of the force profile based on the parameters in Table 1, assuming the outer Helmholtz plane to reside at the

Table 1. Double Layer Parameters Used to Subtract the Long-Range Electrostatic Contribution from All Force Measurements and Summary of Chain Extension as a Function of Rate of Approach

temperature (°C)	rate (nm/min)	electrolyte [$NaNO_3$] (mM)	Debye length κ^{-1} (Å)	surface charge density, σ_e (mC/m^2)
20	3	0.25 ± 0.02	195	1.10
28	4	0.25 ± 0.02	200	1.25
28	0.1	0.25 ± 0.02	200	1.30

lipid headgroup interface, identical to the reference frame for contact, $D = 0$. The electrostatic portion was then subtracted from the force profile, and the remaining repulsive force was attributed to the steric repulsion due to the grafted polymer chains.

For comparison, Figure 4 shows a series of steric force–distance profiles (after subtracting the electrostatic repulsion)

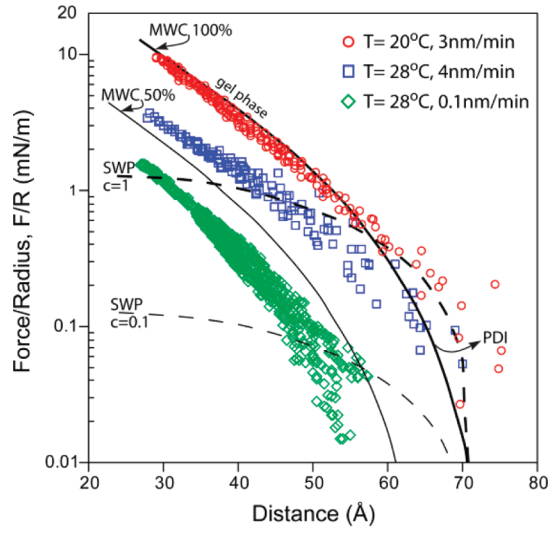

Figure 4. Steric force–distance profiles between bilayers containing 7.5 mol % DMPE-PEG2000 as a function of approach rate. The steric forces were obtained by subtracting the electrostatic double-layer contribution. Approach rate: 3 nm/min at 20 °C (○), 4 nm/min at 28 °C (□), 0.1 nm/min at a 28 °C (◇). The solid curves are fits to the MWC model (eq 2). The solid heavy line indicates MWC fit in the gel-phase case. The thin solid curve represents the MWC model for 1/2 the initial grafting density. The dashed lines are predictions for the SWP model for surfaces bearing mobile polymer chains.

obtained above and below the phase transition temperature of the membrane. Double-layer parameters for each of the experimental conditions are summarized in Table 1. While diffusion is negligible when the membrane is in the solid phase (T < 23.5 °C), this is not true when the membrane is in the fluid phase. Indeed, as the surfaces approach each other, the increase in osmotic pressure provides a directed driving force for the lipopolymer to diffuse out of the contact zone. As a

dx.doi.org/10.1021/la3008552 | Langmuir 2012, 28, 7470–7475

result, the measured electrostatic and steric repulsion when the membrane is in the fluid state will be dependent on the rate of approach and the amount of lipopolymer, if any, that remains between the membranes.

As shown in Figure 4, membrane fluidity clearly results in a decrease in measured repulsion between the membranes, indicating that the amount of lipopolymers present in the contact zone decreased. Both the onset of the repulsion and the magnitude decrease when the membranes are in the fluid phase. A simple back of the envelope calculation can be used to estimate the time for a lipopolymer to diffuse out of the contact zone from $\langle d^2 \rangle = 4D\ \text{time}_{exp}$. As illustrated in Figure 1B, the curvature of the contact zone (here ∼1 cm) and the polymer layer thickness yield an effective distance of ∼15 μm. Using the measured diffusion of PEG-lipids in single supported membranes, D ∼4 $\mu m^2/s$, from Albertorio et al.,[27] the expected time for the lipopolymer to diffuse out of the contact region is only $\text{time}_{exp} \cong 1$ min. Thus, an approach rate of 4 nm/min is sufficient for the lipopolymer to escape from the contact region. Even at a very slow approach rate of 0.1 nm/min, which affords an order of magnitude increase in time_{exp}, lipopolymer clearly remains trapped between the approach surfaces—indicative of hindered diffusion. Kaufmann and co-workers[30] have determined that the mobility of PEG-lipids is reduced for concentrations above 6 mol % due likely to steric interactions of the polymer chains.

One approach to quantify the amount of polymer remaining between the membrane surfaces is to use polymer theory to model the resulting steric repulsion and extract the amount of PEGylated lipid from the theoretical fit to the data. Previous work has shown that the Alexander de Gennes (AdG) theory[36−38] and the self-consistent mean field theory of Milner, Witten, and Cates (MWC) both give a reasonable estimate for the compressive forces of grafted polymer brushes, even for systems that are not in the strongly stretched brush regime.[24,39] In this case, we choose to use the MWC model as an explicit fit to the data without obtaining fitting parameters. Assuming that the brushes have a parabolic profile and do not interdigitate, the force (F) normalized by the curvature of the cylindrical surfaces (R) as a function of separation distance (D), as measured in the SFA, (F/R), can be obtained from MWC theory for the interaction energy between flat interfaces, E, using

$$\frac{F}{R} = 2\pi[E(D) - E(h_o)] = \frac{2\pi h_o kT}{a^3}(a^2\sigma)^{4/3}\left(\frac{w}{a^3}\right)^{1/3}(a^2\nu)^{2/3}\left[\left(\frac{2h_o}{D}\right) + \left(\frac{D}{2h_o}\right)^2 - \left(\frac{D}{2h_o}\right)^5 - \frac{9}{5}\right] \quad (2)$$

where a (=3.5 Å) is the size of a monomer, σ is the area per grafted chain, w is the excluded volume parameter (note: the excluded volume parameter can be found from the osmotic pressure, Π, and volume fraction of PEG monomer in the brush via $\Pi = (1/2)w\phi kT$; at an osmolality c = 55 mol/kg, the osmotic pressure is ∼0.21 MPa, yielding $w = (3.48\ \text{Å})^3 \cong a^3$), ν can be found from $R_F^2 = 3N/\nu$ or the statistical segment length, and the equilibrium extension of the polymer layer, h_o, is given by

$$h_o = \left(\frac{12}{\pi^2}\right)^{1/3} N\cdot a\cdot(a^2\sigma)^{1/3}\left(\frac{w}{a^3}\right)^{1/3}(a^2\nu)^{-1/3} \quad (3)$$

For gel-phase membranes, σ was fixed to the known value of 1 chain/760 Å^2, $w = (3.5\ \text{Å})^3$, and h_o = 38 Å. As shown in Figure 4, MWC provides an excellent fit to the data for D < 60 Å. For small compressions (D > 60 Å), the polydispersity (PDI ∼1.07) of the chains would have to be accounted for to accurately fit the data.[40,41] However, the MWC model is unable to properly account for the fluid-phase membrane force profile data, as the amount of lipopolymer between the membranes changes as a function of separation distance. For comparison, the MWC prediction for a system with a grafting density of 1/2 of the initial concentration (1 chain/1520 Å^2 vs 1 chain/760 Å^2) is shown in Figure 4 (thin solid curve).

A more accurate way to determine the amount of polymer present in the contact zone with fluid membranes is to integrate the area under the curve to obtain total pressure for the contact area. Assuming that the total pressure arises strictly from osmotic repulsion, the Morse equation[42] can be used to relate pressure (Π) and concentration in a straightforward manner

$$\Pi = iMRT \quad (4)$$

where i is the dimensionless van't Hoff factor, M is the molarity, R the gas constant, and T is the temperature. As the polymer concentration in the contact zone is known for the gel-phase case, the ratio of final lipopolymer concentration, M_f, over initial concentration, M_0, can be interpreted as the % lipopolymer remaining at the contact zone, and can easily be obtained from the ratio of the integrated fluid to gel force profiles shown in Figure 4. Table 2 shows that the amount of polymer present in the contact zone decreases as the rate of approach decreases. Indeed at the slowest approach, 87% of the lipopolymer has escaped from the contacting region of the surfaces. A quantitative determination of the diffusion coefficient in this restricted geometry (Figure 1) would require development of the appropriate governing equation based on an osmotic pressure driving force. However, the effective diffusivity can simply be approximated from the contact geometry and measurement time at the slowest approach yielding D < 0.03 $\mu m^2/s$.

Table 2. Estimation of % Polymer Remaining at the Contact Zone[a]

rate (nm/min)	% polymer remaining at the contact zone	elapsed time (min)
3	100	N/A
4	45 ± 5	1.5 ± 0.5
0.1	13 ± 3	30 ± 3

[a]Elapsed time starts when steric repulsion arising from the polymer layer is detected upon approach and ends when surface separation is initiated.

With regard to quantifying the experimentally measured steric force, Subramanian, Williams, and Pincus (SWP) provide an estimate of the total free energy when a surface bearing grafted but mobile polymer chains in the mushroom regime is compressed by a bare disk of area A_1.[43,44] In their scaling model, the total free energy consists of two components: the energy to compress the mushrooms and translational entropic terms that account for the change in the initially, uniform grafting density, $\sigma = \sigma_0$, as chains leave the region under the

dx.doi.org/10.1021/la3008552 | Langmuir 2012, 28, 7470−7475

disk, $\sigma \rightarrow \sigma_1$, and move into the surrounding membrane, $\sigma \rightarrow \sigma_2$. Assuming that the system is always at equilibrium and in the limit of low grafting density, $\sigma_0 R_F^2 \ll 1$, the free energy is minimized with respect to the density of chains under the disk, σ_1, and one finds

$$E = c\sigma_0 kTA_1\left[e^{-(L/D)^{5/3}}\right] \tag{5}$$

where L is the equilibrium, uncompressed extension of the chains, and c is a numerical prefactor. Accounting for the geometry of the SFA and both surfaces having grafted chains yields:

$$\frac{F}{2\pi R} = \frac{E}{A_1} = c\sigma_0 kT\left[e^{-1} - e(2L/D)^{5/2}\right] \qquad D \leq 2L \tag{6}$$

The SWP model with c = 0.1 and 1 is shown in Figure 4. Although the SWP model assumes an isolated mushroom steric contribution to the total energy, which is not appropriate for the conditions used in this work, some general comparisons can be made. First, in the model the repulsion raises rapidly as some compression of the layer is required to drive the chains from the confined region and overcome the pressure forcing mushrooms back under the disk. However, this "ideal gas" pressure is apparently below the experimental resolution, as no detectable steric force is observed at the slowest compression rate until D < 60 Å is significantly less than the measured extension of the brush, $2L \approx 70$ Å. With further compression, the steric force rapidly rises due to confinement but plateaus as the osmotic pressure provides a sufficient driving force to push chains from the confinement region into the bulk (nonconfined region). In the experiments, lipopolymers are clearly driven out of the contact zone for modest compressions. However, a critical compression and resulting plateau in the force is not seen in the experiments—rather, the force rises rapidly for separation distances below ~55 Å. These observations suggest that the diffusion of chains out of the contact zone becomes limited as the surface separation approaches the grafted chain radius of gyration. Given the expected, rapid diffusivity of the lipopolymers (~4 μm^2/min), the trapping of chains in the compression region during the slowest compression implies that equilibrium during the compression was not maintained in the experimental system. Unfortunately, slower compression rates become prohibitive due to potential experimental drift. Although more complicated expressions for the steric force, e.g., MWC, could be used in the SWP model and may more accurately represent the experimental system, the stringent requirement of equilibrium is difficult to achieve.

In closing, direct measurement of the steric repulsion between membranes with embedded lipopolymers demonstrates that the amount of lipopolymer in the contact region is modulated when the membranes are in the fluid phase. The steric repulsion between the membranes decreases as a function of the approach rate due to osmotic pressure driven diffusion. Although a sufficiently slow approach should allow all lipopolymers to be depleted from the contact zone, we find that the diffusivity is significantly retarded, and it is unlikely that equilibrium is maintained during the compression. Still, these findings imply potential avenues to improve targeted drug delivery vehicles. First, the steric barrier afforded by the embedded lipopolymers is critical to maintain circulation times by preventing nonspecific protein absorption. The steric barrier afforded by the embedded lipopolymers is still substantial even in fluid membrane systems. Second, at contact with another surface, these lipopolymers can be driven out of the contact zone if the membrane is fluid, thereby reducing the repulsion between the surfaces. Thus, an ideal scenario for drug delivery applications would involve a small percentage of ligated long-chain lipopolymers in a forest of unligated "steric" bumpers to provide adhesion to the target surface while maintaining a strong steric barrier. The total amount of lipopolymers and the approach rate determines the magnitude of steric repulsion, while the inclusion of ligated lipopolymers can ensure that the contact/adhesion between the surfaces is maintained. Subsequently, the adhesion between the surfaces could be further augmented by an under-layer of short, ligated chains buried in the longer-chained steric forest. Such a tiered system could provide robust steric repulsion that is converted to robust adhesion as the steric barrier presenting lipopolymers are excluded from the contact zone. Experimental measurements probing such tiered structures are currently underway.

AUTHOR INFORMATION

Corresponding Author

*E-mail: tlkuhl@ucdavis.edu.

Notes

The authors declare no competing financial interest.

ACKNOWLEDGMENTS

The authors thank Dennis Mulder and Paul Bulkley-Logston for providing support in automating the Surface Force Apparatus and to Shari Williams for assisting in Langmuir monolayer experiments. This work was performed at UC Davis with support from NSF DMR-0606564. R.O.A. was partially supported by a Designated Emphasis in Biotechnology Fellowship.

REFERENCES

(1) Knop, K.; Hoogenboom, R.; Fischer, D.; Schubert, U. S. Poly(ethylene glycol) in Drug Delivery: Pros and Cons as Well as Potential Alternatives. *Angew. Chem., Int. Ed.* **2010**, *49* (36), 6288−6308.

(2) Wischerhoff, E.; et al. Controlled Cell Adhesion on PEG-Based Switchable Surfaces. *Angew. Chem., Int. Ed.* **2008**, *47* (30), 5666−5668.

(3) Jokerst, J. V.; et al. Nanoparticle PEGylation for imaging and therapy. *Nanomedicine* **2011**, *6* (4), 715−728.

(4) Smet, M. Biological and Medical Applications of Hyperbranched Polymers. In *Hyperbranched Polymers: Synthesis, Properties, and Applications*, Deyue Yan, C. G., Frey, H. , Ed.; John Wiley & Sons, Inc.: Hoboken, NJ, 2011; pp 387−412.

(5) Ferrara, K.; Pollard, R.; Borden, M. Ultrasound microbubble contrast agents: fundamentals and application to gene and drug delivery. *Annu. Rev. Biomed. Eng.* **2007**, *9*, 415−47.

(6) Lasic, D. D. Novel applications of liposomes. *Trends Biotechnol.* **1998**, *16* (7), 307−321.

(7) Wong, J.; Kuhl, T.; Israelachvili, J. N.; Mullah, N.; Zalipsky, S. Direct measurement of a tethered ligand-receptor interaction potential. *Science* **1997**, *275* (5301), 820−822.

(8) Kenworthy, A. K.; Simon, S. A.; McIntosh, T. J. Structure and phase behaviour of lipid suspensions containing phospholipids with covalently attached poly(ethylene glycol). *Biophys. J.* **1995**, *68* (5), 1903−1920.

(9) Lee, C.-M.; et al. Polyethylene Glycol (PEG) Modified 99mTc-HMPAO Liposome for Improving Blood Circulation and Biodistribution: The Effect of the Extent of PEGylation. *Cancer Biother. Radiopharm.* **2005**, *20*, 620−628.

(10) Immordino, M. L.; Dosio, F.; Cattel, L. Stealth liposomes: review of the basic science, rationale, and clinical applications, existing and potential. *Int. J. Nanomed.* **2006**, *1* (3), 297−315.
(11) Vert, M.; Domurado, D. Poly(ethylene glycol): protein-repulsive or albumin-compatible? *J. Biomater. Sci., Polym. Ed.* **2000**, *11*, 1307−17.
(12) Kenworthy, A. K.; Hristova, K.; Needham, D.; McIntosh, T. J. Range and magnitude of the steric pressure between bilayers containing phospholipids with covalently attached poly(ethylene glycol). *Biophys. J.* **1995**, *68* (5), 1921−1936.
(13) Efremova, N. V.; Huang, Y.; Peppas, N. A.; Leckband, D. E. Direct measurements of interactions between thethered poly(ethylene glycol) chains and adsorbed mucin layers. *Langmuir* **2002**, *18* (3), 836−845.
(14) Evans, E.; Leung, A.; Hammer, D.; Simon, S. Chemically distinct transition states govenrn rapid dissociation of single L-selectin bonds under force. *Proc. Natl. Acad. Sci. U.S.A.* **2001**, *98* (7), 3784−3789.
(15) Moore, N. W.; Kuhl, T. L. The role od flexible tethers in multiple ligand-receptor bond formation between curved surfaces. *Biophys. J.* **2006**, *91* (5), 1675−1687.
(16) Moore, N. W.; Kuhl, T. L. Bimodal Polymer Mushrooms: Compressive Forces and Specificity toward Receptor Surfaces. *Langmuir* **2006**, *22*, 8485−8491.
(17) Moore, N. W.; Mulder, D. J.; Kuhl, T. L. Adhesion from Tethered Ligand-Receptor Bonds with Microsecond Lifetimes. *Langmuir* **2008**, *24*, 1212−1218.
(18) Terada, T.; Iwai, M.; Kawakami, S.; Yamashita, F.; Hashida, M. Novel PEG-matrix metalloproteinase-2 cleavable peptide-lipid containing galactosylated liposomes for hepatocellular carcinoma-selective targeting. *Controlled Release* **2006**, *111*, 333−342.
(19) Hussain, S.; Pluckthun, A.; Allen, T. M.; Zangemeister-Wittke, U. Chemosensitization of carcinoma cells using epithelial cell adhesion molecule−targeted liposomal antisense against bcl-2/bcl-xL. *Mol. Cancer Ther.* **2006**, *5* (11), 3170−3180.
(20) Krown, S. E.; Northfelt, D. W.; Osoba, D.; et al. Use of liposomal anthracyclines in Kaposi's sarcoma. *Semin. Oncol.* **2004**, *31*, 36−52.
(21) Rose, P. G. Pegylated liposomal doxorubicin: optimizing the dosing schedule in ovarian cancer. *Oncologist* **2005**, *10*, 205−14.
(22) Mufamadi, M. S. A Review on Composite Liposomal Technologies for Specialized Drug Delivery. *J. Drug Delivery* **2011**, 2011.
(23) Kuhl, T. L.; Leckband, D. E.; Lasic, D. D.; Israelachvili, J. N. Modulation of Interaction Forces Between Bilayers Exposing Short-Chained Ethylene Oxide Headgroups. *Biophys. J.* **1994**, *66*, 1479−1487.
(24) Kuhl, T. L.; Leckband, D. E.; Lasic, D. D.; Israelachvili, J. N. Modulation and Modeling of Interaction Forces Between Lipid Bilayers Exposing Terminally Grafted Polymer Chains. In *Stealth Liposomes*, Lasic, D., Frank, M., Eds.; CRC Press: 1995; pp 73−91.
(25) Kaneshina, S.; et al. Partitioning of local anesthetic dibucaine into bilayer membranes of dimyristoylphosphatidylcholine. *Colloids Surf., B: Biointerface* **1997**, *10*, 51−57.
(26) Tamm, L. K.; McConnell, H. M. Supported Phospholipid Bilayers. *Biophys. J.* **1985**, 47.
(27) Albertorio, F.; Diaz, A. J.; Yang, T.; Chapa, V. A.; Kataoka, S.; Castellana, E. T.; Cremer, P. S. Fluid and Air-Stable Lipopolymer Membranes for Biosensor Applications. *Langmuir* **2005**, *21*, 7476−7482.
(28) Israelachvili, J. N.; Adams, G. E. Measurement of Forces between Two Mica Surfaces in Aqueous Electrolyte Solutions in the Range 0−100 nm. *Chem. Soc., Faraday Trans.* **1978**, *74*, 975−1001.
(29) Israelachvili, J. Thin film studies using multiple beam interferometry. *J. Colloid Interface Sci.* **1973**, *44*, 259.
(30) Kaufmann, S.; Borisov, O.; Textor, M.; Reimhult, E. Mechanical Properties of mushroom and brush poly(ethylene glycol)-phospholipid membranes. *Soft Matter* **2011**, *7*, 9267−9275.
(31) Marra, J.; Israelachvili, J. Direct Measurements of Forces between Phosphatidylcholine and Phosphatidylethanolamine Bilayers in Aqueous Electrolyte Solutions. *Biochemistry* **1985**, *24*, 4608−4618.
(32) Kuzmenka, D. J.; Granick, S. Collapse of poly(ethylene oxide) monolayers. *Macromolecules* **1988**, *21* (3), 779−782.
(33) Ritchie, T. K., et al. Reconstitution of membrane proteins in phospholipid bilayer nanodiscs. In *Methods in Enzymology*, Duzgunes, N., Ed.; Elsevier Inc: 2009; Vol. *464*, Chaper 11, pp 211−231.
(34) Szleifer, I. Statistical thermodynamics of polymers near surfaces. *Curr. Opin. Colloid Interface Sci.* **1996**, 416−423.
(35) Grabbe, A.; Horn, R. G. Double-Layer and Hydration Forces Measured between Silica Sheets Subjected to Various Surface Treatments. *J. Colloid Interface Sci.* **1993**, *157* (2), 375−383.
(36) Alexander, S. Adsorption of chain molecules with a polar head, a scaling desciption. *J. Phys. (Paris)* **1977**, *38*, 983.
(37) de Gennes, P. Polymer solutions near an interface. I. Adsorption and depletion layers. *Macromolecules* **1981**, *14*, 1637.
(38) de Gennes, P. Polymers at an interface; a simplified view. *Adv. Colloid Interface Sci.* **1987**, 27.
(39) Efremova, N. V.; Bondurant, B.; O'Brien, D. F.; Leckband, D. E. Measurements of interbilayer forces and protein adsorption on uncharged lipid bilayers displaying poly(ethylene glycol) chains. *Biochemistry* **2000**, *39* (12), 3441−3451.
(40) Milner, S. T. Compressing Polymer "Brushes": a Quantitative Comparison of Theory and Experiment. *Europhys. Lett.* **1988**, *7* (8), 695−699.
(41) Alonzo, J. M.; Kilbey, S. M., II Forces of interaction between surfaces bearing looped polymer brushes in good solvent. *Soft Matter* **2009**, *5*, 1897−1904.
(42) Amiji, M. M., Sandmann, B. J. Physical Properties of Solutions. In *Applied Physical Pharmacy*, Brown, M., Sheinis, L. A., Eds.; McGraw-Hill Companies, Inc.: New York, 2002; pp 55−56.
(43) Subramanian, G.; Williams, D. R. M.; Pincus, P. A. Interaction between Finite-Sized Particles and End Grafted Polymers. *Macromolecules* **1996**, *29*, 4045−4050.
(44) Subramanian, G.; Williams, D. R. M.; Pincus, P. A. Escape Transitions and Force Laws for Compressed Polymer Mushrooms. *Europhys. Lett.* **1995**, *29* (4), 285−290.